

in the inner fan-valley, and 26 m/km along the Monterey submarine canyon.

An impressive levee along the convex side of the meander rises locally as much as 380 m above the channel floor and as much as 100 m above the surrounding fan. A profile along the top of this levee (Fig. 2) contrasts markedly with that of the channel. The levee profile shows a series of rises and sags. The largest sag along the top of the levee is near the southern extreme of the meander, and this sag connects it with a discontinuous valley extending farther south (Fig. 1). The latter contains a large basin depression. The plateau on the inside of the meander has rolling topography with a group of small hills. None of these hills rises as high as the highest parts of the outer levee on the west side of the meander. An echosounding profile across the entire feature is shown in Fig. 2.

A total of 18 samples was taken in the area of the meander. These were mostly box cores, which are obtained in a rectangular box 20 by 30 cm in ground plan and 40 cm high on a frame with a pivotal closing mechanism which retains the core (4). Gravity cores up to 2 m in length were also included. These samples were obtained from the slopes, from the levee that conforms to the outer bend, from the high ground inside the meander, and from the discontinuous channel south of the meander. In all except the valley slope sam-

ples, sand layers or sand lenses were found. The sand is well sorted and mostly fine-grained but includes some medium-grained sand on the levee east of the meander. The two gravity cores on the slope were entirely mud.

Before drawing more than tentative conclusions, additional information must be found. Perhaps the most reasonable interpretation of the feature is that the entire fan-valley was produced by turbidity currents moving across the fan and entrenching a valley into it. Study of the fan-valley seaward of La Jolla Canyon shows that cutting is taking place on the outside of the bends in the channels (5), and one can suppose that such cutting has produced the meander off Monterey. The thickness of the occasional turbidity currents moving down the channel can be inferred to be as much as 380 m in order to build up the top of the west levee. It is also significant that these thick flows were transporting sand when they spilled over the levees. Judging from our experience in observing currents from Cousteau's Diving Saucer (6), it would seem reasonable that the current necessary to transport this sand would be at least one-half knot (25 cm/sec). Presumably, the current was much stronger along the floor of the valley.

Perhaps the most puzzling feature about the meander is that it is only along this short stretch of the fan-valley that the axis has such a trend (Fig. 1). The entire fan-valley has been traced for

about 170 km beyond Monterey Canyon. The upper portion is relatively straight, and the lower portion is slightly sinuous but has no true meander. Possibly the meander is related to some underlying structure, perhaps a coarse sediment zone in the underlying fan deposits.

FRANCIS P. SHEPARD

*Scripps Institution of Oceanography,  
University of California, San Diego*

#### References and Notes

1. F. P. Shepard, *Bull. Am. Ass. Petrol. Geol.* 49, 304 (1965).
2. R. F. Dill, R. S. Dietz, H. B. Stewart, Jr., *Bull. Geol. Soc. Am.* 65, 191 (1954).
3. P. Wilde, *Am. Soc. Limnol. Oceanog.* 2, 718 (1965).
4. H. E. Reineck, *Natur. Museum* 93, 65 (1963).
5. D. G. Moore, *Bull. Geol. Soc. Am.* 76, 385 (1965).
6. F. P. Shepard, in *Submarine Geology and Geophysics*, W. F. Whittard and R. Bradshaw, Eds. (Butterworths, London, 1965), pp. 303-311.
7. Supported in part by ONR contract Nonr-2216(23) and NSF grant GP-3601.

31 August 1966

#### Generation of Light from Free Electrons

Abstract. *Experiments with the interaction of a rectangular cross-section beam of electrons which is brought into contact with a metallic diffraction grating produce light variable in wavelength throughout the visible spectrum. Continuous variation of the beam thickness shows that light is produced by electrons hundreds of wavelengths from the grating, if the side of the beam near the grating is in contact with it. The results can be accounted for by periodic accelerations of the electrons passing over the surface of the grating. These accelerations are caused by electrostatic forces which in turn are due to the average space-charge of sheets of electrons reflected from the grating surface, so that in their space-charge structure the periodicity of the grating rulings is preserved.*

The suggestion that visual light (Fig. 1) could be generated by the interaction of a beam of electrons with a metallic diffraction grating was made in 1949 (1). Independently, Smith and Purcell (2) described an experiment confirming this effect and proposed that an electrostatic image model of induced surface charges moving over the ruled grating surface could account for the observed radiation.

I have now carried out experiments

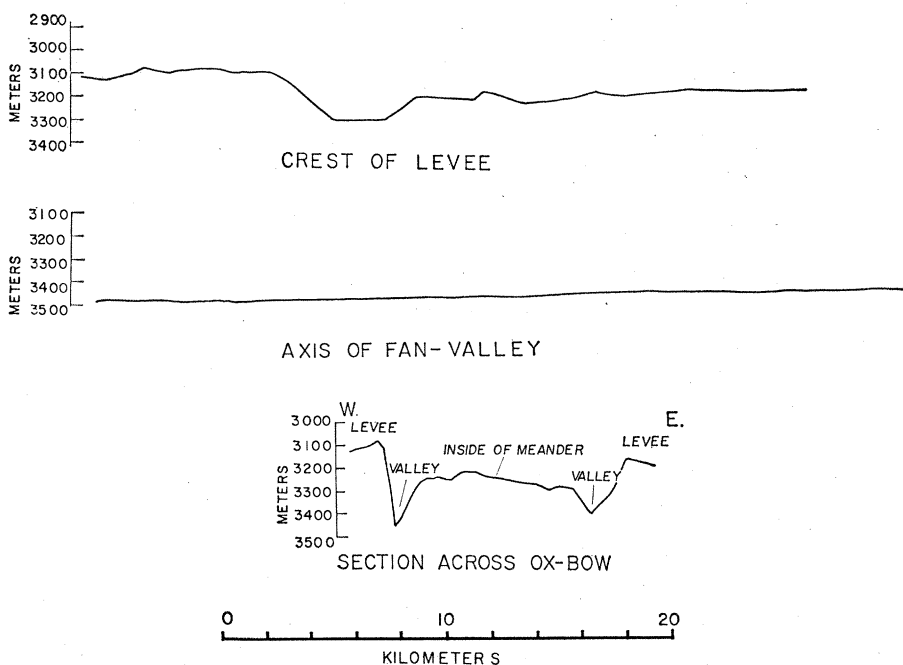


Fig. 2. Profiles along crest of levee, along the axis of fan-valley, and from a fathogram across the southern end of the meander. All profiles have same scale.

intended to determine more fully the limits of the parameters involved in this effect. This work led to unexpected results, and to the proposal of a new mechanism: that reflected electrons produce space-charge sheets having the spacing characteristics of the grating, and that electrons passing through these sheets undergo accelerations which produce radiation.

A sharply defined beam of electrons was produced so that the energy of the electrons could be varied in the region from 25 to 250 kev. The beam was defined by a series of well-aligned double slits constructed to minimize scattering from the jaws. The beam used in most experiments was about 1/4 mm thick and 3 mm wide (Fig. 2). Observations made with this apparatus confirm the observations of Smith and Purcell in respect to the wavelength of the emitted radiations and the existence of harmonics. The wavelengths of the observed radiation can be expressed by a simple Doppler equation as if the source of radiation were moving with the velocity of the electrons, as

$$\lambda = D(\beta^{-1} + \cos \theta),$$

where  $\lambda$  is the observed wavelength,  $D$  is the grating ruling space,  $\beta$  is the ratio

of the electron velocity to the velocity of light, and  $\theta$  is the angle between the line of sight of the observer and the velocity vector of the electrons.

The theory that induced surface charges moving over the grating were the source of radiation has been extensively studied (3). In all of these studies it is agreed that, on the assumption of surface-charge action, electrons must be moving approximately parallel to the grating surface at a distance of no greater than a few grating-line spacings in order to produce visible radiation.

This assumption was tested experimentally by making the upper jaw of the final electron slit movable, perpendicular to the thickness of the electron beam. Movement of this jaw can then produce a thinner and thinner electron beam so that if the beam is initially grazing the grating, the electrons that pass the grating far away are gradually cut out of the beam. This operation showed that the light intensity varied linearly with the beam thickness. Electrons, hundreds of ruling spacings away, thus produce as much light as those close to the grating. This observation is completely contrary to the idea of surface current radiation. An addi-

tional accidental observation agrees with this finding. Operation in a vacuum containing some residual oil from a diffusion pump produced a carbon coating over the grating where the electron beam passed by. This coating became optically thick enough to stop reflection of light from the grating surface, and hence thick enough to mask any surface currents of visual frequency. (Such currents are a required part of reflection as well as surface radiation; see Maxwell's equations.) Nevertheless, the radiation produced by the electrons was unaffected.

A metallic diffraction grating was mounted on micrometers in the vacuum chamber with the electron beam. The electron slits and accelerating fields were arranged so that the space where the electrons interact with the grating was essentially free from electrostatic fields. The grating could be moved to come into parallel contact with the beam surface, with the velocity vector of the electrons essentially perpendicular to the grating rulings.

A movement of the grating of about 3  $\mu$ , perpendicular to the electron beam, is sufficient to progress from a position at which there is essentially no contact with the electrons, to a position which

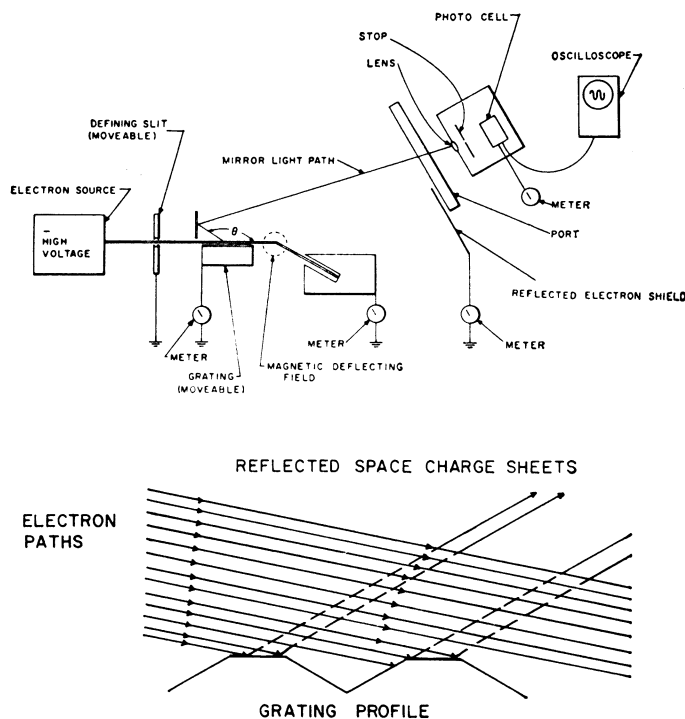
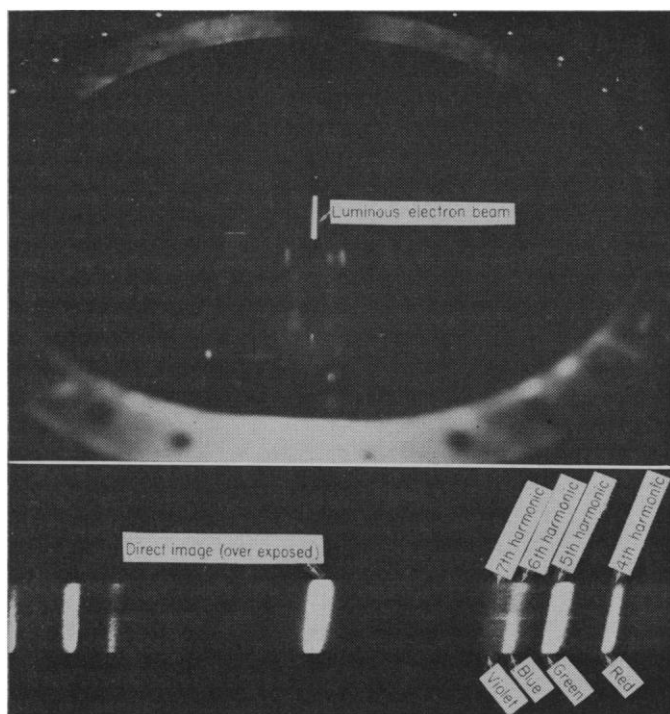


Fig. 1 (top left). Electron beam radiating green light, vertical bright bar in center of picture (1/50th-second exposure ectochrome color film with flood lights). Fig. 2 (top right). Schematic drawing of apparatus used in passing an electron beam over a diffraction grating to produce light. Fig. 3 (bottom left). Light produced by electron beam and diffraction grating as seen through a transmission grating. Four spectral images appear on each side of the central image. The colors in the original color photograph of the spectral image are, starting from the outside in sequence inward, red, green, blue, and violet. They represent the 4th, 6th, and 7th harmonics of the Fourier series representing the grating profile. Fig. 4 (bottom right). Electron space-charge interference pattern (electron angles exaggerated). Proposed mechanism for the generation of light by space-charge sheets.

causes the electrons to emit light and causes a current (which is small compared to that of the electron beam) to be picked up by the grating. This small required movement shows the sharp definition of the edges of the electron beam.

Adjustment of the grating position showed that some electrons must strike the grating in order to produce light. This was investigated by means of an electrode introduced above the beam to catch electrons which ricochet from the grating at near-grazing incidence. Measurements of the current of reflected electrons showed that some reflected current was required to produce light and that the light intensity is proportional to this current. Measurements of the electron current passing the grating in a straight line show that the light intensity is proportional to this current also. The light intensity is thus proportional to the product of the current reflected from the grating and the undeflected current passing the grating. This proportionality has been tested for total currents of a fraction of a microampere, where the light is just visible, through the range of a few tens of microamperes, where light is visible in a well-lit room, up to about 10 ma where the light seems very bright.

Many different grating profiles and grating spacings were used in various observations. Grating line densities ranging from 4000 to 30,000 per centimeter were used.

The principal significant effect of the grating profile used is that light generated with a grating having flats between the rulings is rich in harmonics. A photograph made with a simple spectroscope, consisting of an auxiliary transmission grating, shows the fourth, fifth, sixth, and seventh harmonic of a fundamental which is in the far infrared. The four harmonics shown are in the visual portion of the spectrum (Fig. 3).

A simple explanation of this radiation is proposed here. As is well known, periodic acceleration of electrons produces electromagnetic radiation. The electrons reflected from the grating are believed to form sheets of space-charge having the same periodicity as the grating. Other electrons passing through these sheets of space-charge are alternately accelerated and decelerated by the electrostatic forces between them and the electrons in space-charge sheets. This periodic acceleration causes radiation from electrons that may be far

from the grating surface (Fig. 4). This radiation in no way depends on surface currents in the grating. Low-density carbon deposits on the grating which are opaque to light will have no appreciable effect on high-energy electrons passing through them, because of the thinness and low density of the deposits.

WINFIELD W. SALISBURY  
*Smithsonian Astrophysical Observatory,  
Harvard College Observatory,  
Cambridge, Massachusetts*

#### References and Notes

1. W. W. Salisbury, Patent No. 2,634,372, 26 October 1949.
2. S. J. Smith and E. M. Purcell, *Phys. Rev.* **92**, 1069 (1953).
3. C. W. Barnes and K. G. Dedrick, *J. Appl. Phys.* **37**, 411 (1966); G. Toraldo di Francia, *Nuovo Cimento* **16**, 61 (1960), I. Palocz, thesis, Polytechnic Institute of Brooklyn; Ann Arbor, University Microfilms (1962); I. Palocz and A. A. Oliner, Research Paper RC-1243, Brooklyn Polytechnic Institute, 30 July 1964; A. Hessel, Research Report No. TIBMRI-825-60, Air Force Cambridge Research Laboratories, 2 December 1963.
4. Supported in part by Varo, Inc., Garland, Texas; and in part by the U.S. Air Force.

25 August 1966

### Pressure-Induced Dehydration Reactions and Transitions in Inorganic Hydrates

*Abstract. Application of high pressure at 25°C irreversibly dehydrated five inorganic compounds containing molecular water to lower hydrates or to anhydrous forms. Compression at 25°C also lead to ten new reversible phase transformations in another group of nine hydrates. Maximum pressure applied was 22.6 kilobars.*

There has been no concerted attempt so far to dehydrate inorganic compounds containing molecular water by compression alone. Bridgman *et al.* (1), while trying to produce stress minerals, accidentally dehydrated gypsum and opal. Kiyama and Yanagimoto (2) dehydrated  $\text{CuSO}_4 \cdot 5\text{H}_2\text{O}$ , and Levshits *et al.* (3) removed water from  $\text{MgSO}_4 \cdot 7\text{H}_2\text{O}$  by applying high pressures and temperatures. We compressed inorganic hydrates to a maximum pressure of 22.6 kb at 25°C and found complete dehydration in  $\text{Na}_2\text{SO}_3 \cdot 7\text{H}_2\text{O}$  at 8.9 kb,  $\text{ThCl}_4 \cdot 8\text{H}_2\text{O}$  over a range of 2.2 to 4.6 kb, and partial dehydration of  $\text{ZnSO}_4 \cdot 7\text{H}_2\text{O}$  to  $\text{ZnSO}_4 \cdot 6\text{H}_2\text{O}$  at 4.6 kb. Dehydrations of indeterminate character also occurred in  $\text{Ca}(\text{CNS})_2 \cdot 4\text{H}_2\text{O}$  at 0.5 kb, and  $\text{Zr}(\text{SO}_4)_2 \cdot 4\text{H}_2\text{O}$  over a broad range of pressure.

While none of the other nine com-

pounds showed any degree of dehydration, they underwent first-order reversible volumetric transitions. Zinc sulfate heptahydrate and  $\text{ZnSO}_4 \cdot 6\text{H}_2\text{O}$  undergo phase transitions at 2.2 kb and  $\text{ZnSO}_4 \cdot 6\text{H}_2\text{O}$  has another one at 16.2 kb. Sodium thiosulfate pentahydrate changes reversibly into a new phase at 18.5 kb. Magnesium thiosulfate hexahydrate at 7.7 kb,  $\text{K}_2(\text{MoO}_4) \cdot 5\text{H}_2\text{O}$  at 10.3 kb,  $\text{BeSO}_4 \cdot 4\text{H}_2\text{O}$  at 10.3 kb,  $\text{ZrOCl} \cdot 8\text{H}_2\text{O}$  at 5.6 kb,  $\text{Mg}(\text{SCN})_2 \cdot 4\text{H}_2\text{O}$  at 5.8 kb and  $\text{Th}(\text{SO}_4)_2 \cdot 8\text{H}_2\text{O}$  at 9.8 kb have similar phase transformations.

To detect dehydration we used visual evidence of leakage of water from our apparatus, and whenever possible we compared the curves for longitudinal strain versus pressure for the dehydrated compound with the same curves for the actual lower hydrate or anhydrous form. We define  $l_0$  as the length of the sample at atmospheric pressure and  $l$  as the length of the sample at pressure  $P$ ;  $-\Delta l = -(l - l_0)$  and  $\Delta l/l_0$  is the longitudinal strain. Thus similarities in the longitudinal strain-pressure curves (Fig. 1) for  $\text{Na}_2\text{SO}_3 \cdot 7\text{H}_2\text{O}$  and  $\text{Na}_2\text{SO}_3$ ,  $\text{ZnSO}_4 \cdot 7\text{H}_2\text{O}$  and  $\text{ZnSO}_4 \cdot 6\text{H}_2\text{O}$ , and  $\text{ThCl}_4 \cdot 8\text{H}_2\text{O}$  and  $\text{ThCl}_4$  confirmed the dehydration of these compounds, whereas the oozing of moisture from the pressure cylinder during the compression of  $\text{Ca}(\text{SCN})_2 \cdot 4\text{H}_2\text{O}$  and  $\text{Zr}(\text{SO}_4)_2 \cdot 4\text{H}_2\text{O}$  was the only evidence for loss of water in these two compounds. We could not obtain  $\text{Ca}(\text{SCN})_2$  and  $\text{Zr}(\text{SO}_4)_2$  for reference. The first drift of displacement with time and first deviation from continuity on a graph indicated the onset of a reversible phase transformation.

We used a piston cylinder-type assembly for subjecting our material to pressure. A General Electric carboloy 55A cylinder, 1.257 inches in outer diameter, 0.250 inch inner diameter, and 1 inch (2.54 cm) long, reinforced by three shrink-fitted Alco S steel rings, acted as a container for approximately 0.2 g of powdery sample. Two General Electric carboloy grade 883 pistons, 0.249 inch in diameter and 1 inch long, transmitted the pressure from a 200-ton hydraulic ram to the compound in the carbide cylinder. Alco S steel sleeves, 1 inch outer diameter, 0.247 inch inner diameter, and 1/2 inch long, press-fitted on the external part of these pistons, provided support for stress transmission. An automatic temperature controller connected to an electrically heated oil bath maintained the sample